

Metallicity Evolution of Damped Lyman- α Systems

Sandra Savaglio

*Space Telescope Science Institute, 3700 San Martin Drive, Baltimore
MD 21218, USA*

Abstract. According to Pei, Fall, & Hauser (1999), the global metallicity evolution of the Universe can be represented by the ratio of the total metal content to the total gas content measured in damped Lyman- α (DLA) systems (the “column density weighted metallicity” à la Pettini). To minimize dust obscuration effects, a DLA sample with negligible dust content is considered, namely, 50 DLAs with $\log N_{HI} < 20.8$. The global metallicity found shows clear evidence of redshift evolution that goes from $\sim 1/30$ solar at $z \sim 4.1$ to solar at $z \sim 0.4$. More generally, DLAs with measured heavy elements probe the ISM of high redshift galaxies. The whole sample collected from the literature contains 75 DLAs. The metallicity is calculated adopting for the dust correction the most general method used so far, based on models of the ISM dust depletions in the Galaxy. The intrinsic metallicity evolution of DLA galaxies is $d \log Z_{DLA}/dz = -0.33 \pm 0.06$.

1. Introduction

A damped Lyman- α (DLA) system is often referred to as a QSO absorption line system with HI column density larger than 2×10^{20} atoms cm^{-2} associated with clouds in protogalactic disks (Wolfe et al. 1986). In a more modern fashion, DLAs are mostly neutral gas clouds (HI column density larger than $\sim 10^{19}$ atoms cm^{-2}) associated with the interstellar medium (ISM) of a not defined class of galaxies detected from redshift $z = 0$ up to $z = 4.6$. Among others, examples of the variety of morphologies of the emitting counterpart found nearby DLAs are given by Le Brun et al. (1997) and Rao & Turnshek (1998).

The large investment of telescope time dedicated to QSO surveys (Fan et al. 1999) and specifically to DLA surveys (Rao & Turnshek 1999) has brought the discovery of numerous DLAs. We know 180 objects (Fig. 1) and 55 candidates for a total of 235 DLAs in the redshift range $0.0 < z < 4.6$. Among these, 75 are DLAs for which the column density of HI and one or more of the following ions have been measured: FeII, SiII, NiII, MnII, CrII, ZnII. These ions are the dominant contributors to the abundances of the corresponding elements in HI clouds with high column densities, because they all have ionization potentials below 13.6 eV. For this reason it is easy and straightforward to determine the relative heavy element abundance, just using the standard relation $[X/Y] = \log(N_X/N_Y)_{DLA} - \log(X/Y)_{\odot}$. An important contribution to the richness of this

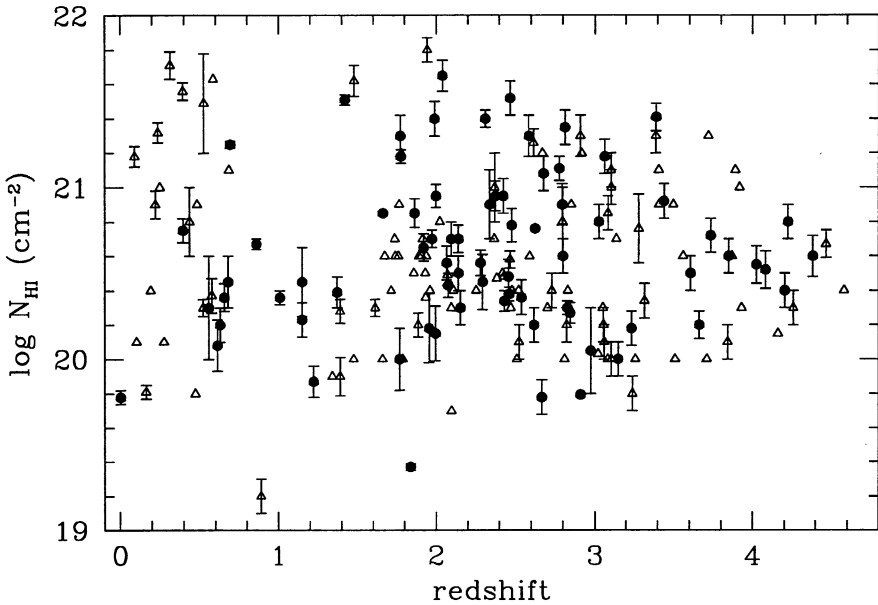


Figure 1. Neutral hydrogen column density for a sample of 180 DLAs in the redshift range $0.0 < z < 4.6$. Dots are DLAs with at least one measured heavy element, triangles are the remaining DLAs. Those points without error bars are DLAs with no HI uncertainty measured.

sample has been provided by Prochaska & Wolfe (1999), Pettini et al. (1997), and Lu et al. (1996). The heavy element enrichment of DLAs has been studied recently in detail by Pettini et al. (1999) and Vladilo et al. (2000) who considered ZnII absorption as a tracer of metallicity, and by Prochaska & Wolfe (2000), who preferred FeII measurements instead. Here we try to show that by combining this information together to build a larger database (75 DLAs at $0.0 < z < 4.4$) and making some assumptions about biases due to dust obscuration, we can have good evidence that the metallicity of the Universe as given by DLAs evolves with cosmic time.

2. Zinc vs. Iron

Very often when discussing metallicity in DLAs, one is actually talking about the abundance of zinc relative to hydrogen. The zinc abundance is considered the right quantity because it suffers very little depletion onto dust grains and because the ZnII doublet is never saturated, and therefore easier to measure with accuracy (Pettini et al. 1994). Other elements like iron are often discarded because they are heavily locked in dust grains.

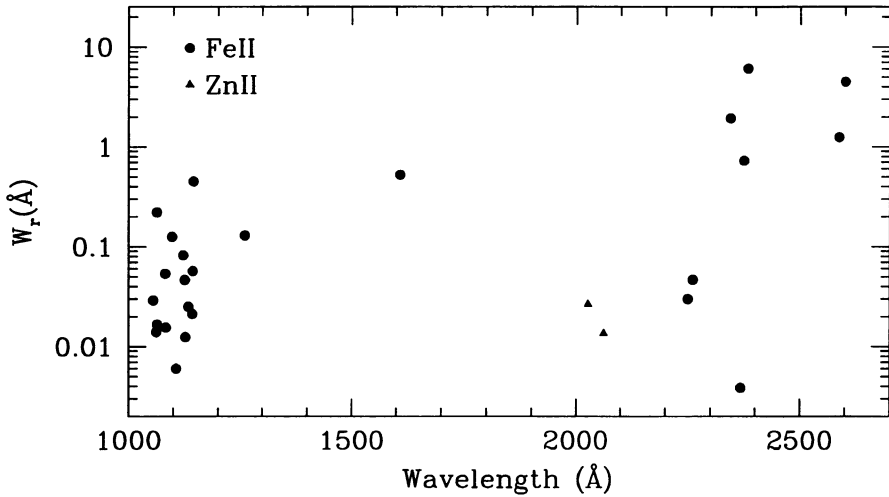


Figure 2. Equivalent widths of FeII and ZnII absorption lines for a DLA with $\log N_{HI} = 20.7$ and metallicity 1/10 solar, as a function of transition wavelength. In this case the relative dust depletion for the two ions is assumed to be $[\text{Fe}/\text{Zn}] = -0.54$ dex.

However, important information is also carried by dust-depleted elements. In Fig. 2 we plot an example of typical equivalent widths in the linear part of the curve of growth (Spitzer 1978) of the ZnII doublet and the multiple lines of FeII as a function of the transition wavelength. These are typical of a DLA system with $\log N_{HI} = 20.7$ and metallicity 1/10 solar. The presence of dust, which makes the iron in the gas phase less abundant relative to zinc, is taken into account assuming a relative dust depletion of $[\text{Fe}/\text{Zn}] = -0.54$. This value is the mean of iron relative to zinc abundance measured in a sample of 27 DLAs.

The FeII ion is characterized by numerous multiplets of lines which absorb in a large wavelength range, while ZnII is just present through a doublet around 2000 Å rest frame. This means that iron can be detected in the optical at the lowest and highest redshifts up to $z \sim 8$, whereas ZnII already approaches the infrared, where spectroscopy is much less sensitive, at $z \sim 3.9$. Another advantage of iron is the oscillator strengths, which vary by three orders of magnitude in different absorption lines, making the detection of the ion very sensitive in very low metallicity DLAs or overcoming the problem of saturation when metallicity is high. Even if the ZnII doublet oscillator strengths are large, the much lower cosmic abundance of zinc with respect to iron (almost three orders of magnitude) make the detection harder when the metallicity is low. FeII in general is much easier to detect because it is less affected by biases. This is shown in Fig. 3, where samples of DLAs with measured FeII and ZnII are reported. In the sample of 75 DLAs, there are 59 objects with FeII in the redshift range $0.0 < z < 4.4$, and 31 objects (almost a factor of two less!) with ZnII in a smaller redshift

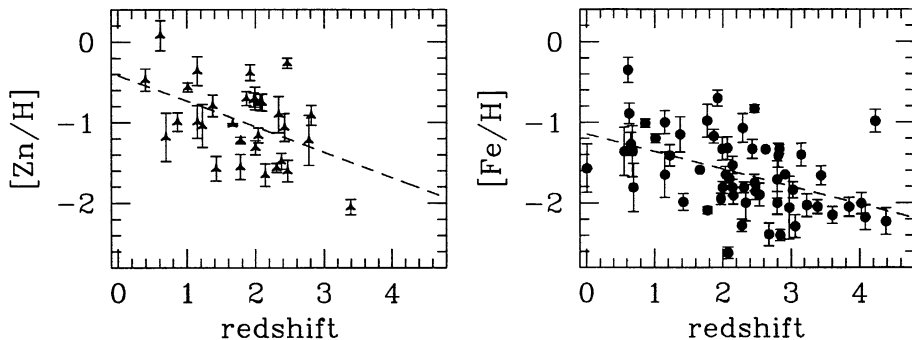


Figure 3. Zinc and iron metallicities as a function of redshift in DLAs. In the first case there are 31 detections at $0.4 < z < 3.4$, while in the second we have 59 at $0.0 < z < 4.4$. Straight lines are the linear correlations for the two cases: $[Zn/H] \propto (-0.32 \pm 0.11) \times z$ and $[Fe/H] \propto (-0.22 \pm 0.06) \times z$.

range $0.4 < z < 3.4$. As a consequence, if only ZnII is considered, the statistics are more limited in redshift range and biased toward low metallicity/dust free DLAs. The selection effects are discussed in more detail in section 5.

3. Dust Depletion Correction and Metallicity Determination

To derive a complete picture of the DLA chemical state, one must consider all detected heavy elements and correct for dust depletion effects. This is not particularly easy since every element is affected differently by dust depletion. In the Milky Way, a number of depletion patterns have been identified, showing highest depletions in dense disk clouds and lowest depletions in low density, warm halo clouds (Savage & Sembach 1996). Although each of the various patterns shows a range of possible depletions (typically within factors of 3), the trends are quite clear and the differences between the various patterns are unambiguously determined. The situation for DLAs may not be clear a priori because one does not know how similar the physical conditions are in the absorbing clouds of different objects, nor whether the nature of dust in different objects is comparable. On the other hand, the similarities of the mean abundance ratios in DLAs with the ones of warm halo clouds and SMC absorbers (Welty et al. 1997; Savaglio, Panagia, & Stiavelli 2000) suggest that the prevailing conditions cannot be very dissimilar. Therefore, we can make a simplification assuming that the depletion patterns in DLAs may be reproduced by one of the four depletion patterns identified for the Milky Way: Warm Halo (WH), Warm Halo + Disk (WHD), Warm Disk (WD) and Cool Disk (CD) clouds (Savage & Sembach 1996), thus modifying the dust-to-metals ratio to obtain the best match to observations.

In practice, let us call J the depletion pattern for which we are comparing the abundance ratios observed in a given DLA. For every element X_i of that DLA, we consider the two quantities:

$$\begin{cases} \delta x_i = [X/H]_{DLA} - \log\left(\frac{Z_{DLA}}{Z_{\odot}}\right) \\ \delta y_i = \log\left[1 + \frac{k_{DLA}}{k_J}(10^{\delta x_i^J} - 1)\right] \end{cases} \quad (1)$$

where $i = 1, 2, 3, \dots$ for S, Zn, Si..., and $J = 1, 2, 3, 4$ for WH, WHD, WD, CD. The quantity δx_i^J is the observed depletion of element X_i in J -type clouds. The two unknowns are the DLA metallicity compared with solar, $\zeta = Z_{DLA}/Z_{\odot}$, and its dust-to-metals ratio κ as compared with that of the J -type clouds: $\kappa = k_{DLA}/k_J$. The values of ζ and κ that minimize the reduced χ^2 :

$$\frac{\chi^2(\kappa, \zeta)}{dof} = \frac{1}{N-2} \sum_i \left[\frac{\delta x_i - \delta y_i}{\sigma(\log X_i)} \right]^2 \quad (2)$$

give the best solution to the problem. Here $N-2$ is the number of degrees of freedom, dof , and $\sigma(\log X_i)$ is the error on the measured column density, $\log X_i$. We have applied this method using the WH, WHD, WD and CD depletion patterns, and for each DLA we obtained four sets of κ and ζ values, from which we select the maximum likelihood solution. As an example, we report in Fig. 4 the depletion pattern of the $z_{DLA} = 1.7688$ absorber along the QSO 0216+0803 sight line (Lu et al. 1996) together with the best solution.

4. Metallicity Evolution

Fig. 5 shows the metallicity as a function of redshift found using this method for the 75 DLAs. Filled symbols represent DLAs with more than two measured element abundances for which it has been possible to obtain a proper best fit solution (38 DLAs). For these, the error bars have been calculated including both the uncertainties in the measured column densities, and the dust model fitting errors. For the cases with only two elements observed, a reduced χ^2 cannot be calculated; thus, the best fit is considered less significant (18 DLAs, empty symbols and solid error bars). In these cases, the error bars include uncertainty in the column densities plus, summed in quadrature, an average error of 0.15 dex, selected for being the mean fitting uncertainty for the DLAs with more than two measured elements. Finally, for the cases where only one element is measured, we only tentatively give an estimate of the metallicity assuming a WH depletion pattern (this is the most likely case, given the global properties) with $\kappa = 1$ (19 DLAs, empty symbols and dotted error bars). In these cases, the error bars include an additional 1.5×0.15 dex that takes into account the fitting uncertainty, and this is larger than derived for 92% of the DLA sample with more than two measured elements.

The mean metallicity calculated for the whole sample is $\langle Z_{DLA}/Z_{\odot} \rangle \simeq 0.1$ and the mean redshift $z_{DLA} \simeq 2.27$. In Fig. 5 we also show six boxes, centered on the weighted averages over $\Delta z = 0.74$ intervals. Their vertical widths mark the corresponding $\pm 1\sigma$ weighted dispersion. We note that the

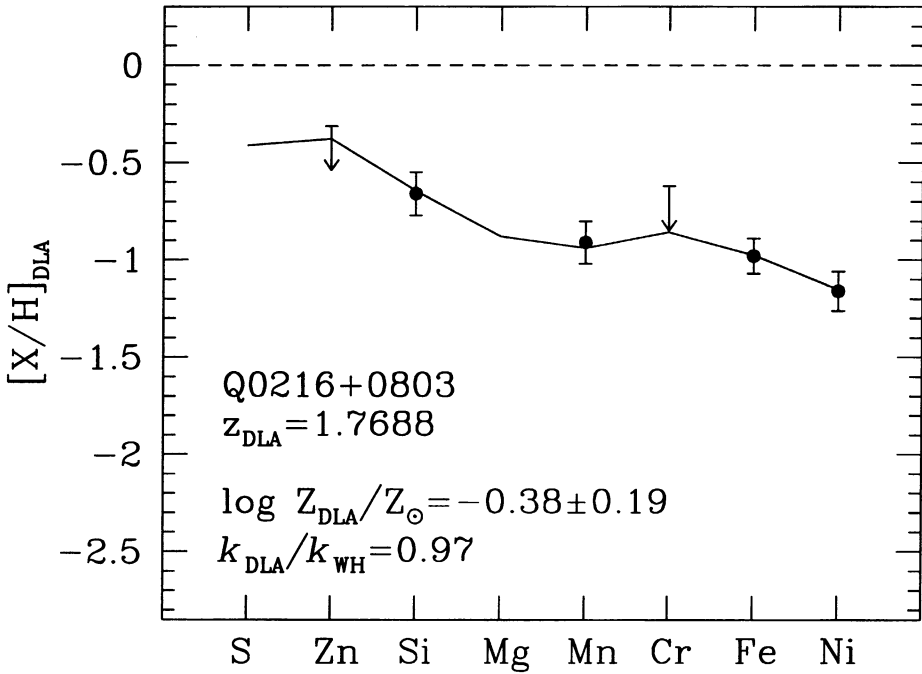


Figure 4. Metallicity measurement for the DLA at redshift 1.7688 along the QSO 0216+0803 sight line. The maximum likelihood solution gives in this case a metallicity of about 2/5 of solar and a WH depletion pattern with dust-to-metals ratio very similar to that of the WH clouds.

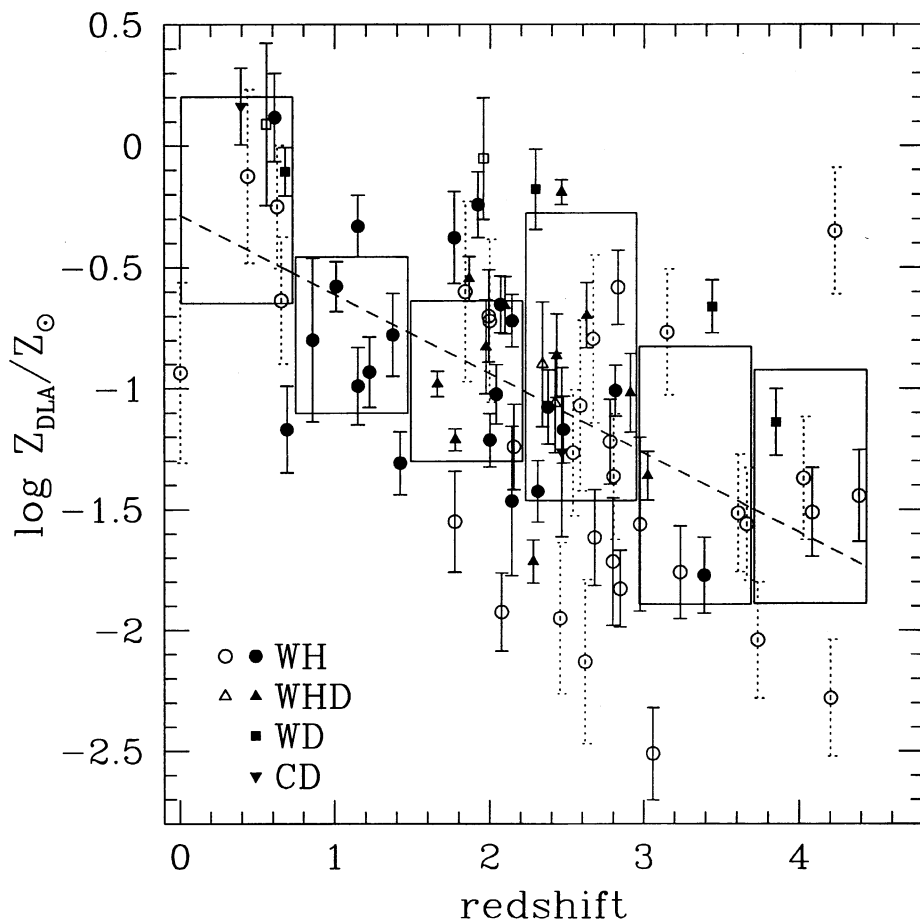


Figure 5. Total (gas+dust) metallicity compared to solar for 75 DLAs. For 38 objects (filled symbols) the dust correction and metallicity measurements are the result of a full χ^2 minimization. Open symbols are DLAs with two elements (solid bars, 18 objects) or one element (dotted bars, 19 objects) measured. The dashed line is the best fit for the whole sample in the case of linear correlation: $d \log Z_{DLA}/dz \simeq -0.33$. Boxes are centered on the weighted averages over $\Delta z = 0.74$ intervals and vertical widths mark the corresponding $\pm 1\sigma$ weighted dispersion.

vertical dispersion of the points, 0.49 dex, greatly exceeds the mean error of 0.20 dex. This indicates that, although DLAs follow an average trend, there are real differences among individual objects in either initial conditions, or time of formation, or metal enrichment efficiency, or all of the above. To see whether there is a redshift gradient of metallicity, we applied the Spearman test to the whole sample and find a correlation coefficient of -0.57 (99.99% significance level). The combination of the largest sample available (75 DLAs), a large redshift baseline ($0.0 < z < 4.4$) and a more accurate dust correction have led to the unambiguous detection of the redshift evolution of metallicity in DLA galaxies, with mean values around 1/25 of solar at $z \sim 4.1$ to 3/5 of solar at $z \sim 0.5$. If a linear correlation is assumed between metallicity and redshift, we find a slope of $d \log Z_{DLA}/dz = -0.328 \pm 0.057$. To test if this result is robust, we have calculated the linear correlation for the sample of 38 DLAs with more than two measured elements and found consistent results ($d \log Z_{DLA}/dz = -0.266 \pm 0.085$, 99.65% significance level).

5. Dust Extinction in DLA QSOs

In Fig. 6 we show a plot of $[Zn/H]$ vs. $\log N_{HI}$ – originally presented by Boissé et al. (1998) – for a sample of 31 DLAs. DLAs with high $[Zn/H]$ abundances and high HI column densities are not detected. These are the DLAs with larger dust content and are therefore harder to observe due to dust extinction. In fact, obscuration at Lyman- α , calculated assuming an SMC-like extinction law directly proportional to the column density of metals, is $A_{Ly\alpha} > 1$ mag for a ZnII column density $\log N_{ZnII} > 13$. In other words, dust obscuration can play an important role, in particular when considering ZnII selected DLAs because ZnII absorption is harder to detect than that of FeII (see Fig. 2).

The effect of dust obscuration is also shown in Fig. 7, where the metallicity of high N_{HI} DLAs is displayed more clearly as a function of redshift. High N_{HI} DLAs are detected only when the metallicity is low. The horizontal lines indicate three metallicities and HI column densities necessary to have an extinction $A_{Ly\alpha} = 1$ mag. There are no DLAs with $\log N_{HI} > 21$ at low redshifts. This means that if there is a metallicity evolution of DLAs, it is difficult to detect in a sample of high N_{HI} DLAs because the dust content, which is proportional to metallicity, and thus the dust obscuration, is larger.

To better understand a possible dependence on the DLA gas content, we applied the metallicity analysis to the two subsamples of DLAs with low ($\log N_{HI} \leq 20.3$, 20 DLAs) and high ($\log N_{HI} \geq 20.9$, 20 DLAs) HI column densities (Fig. 8). What can clearly be noticed is a completely different redshift distribution in the two samples due to observational effects. The low N_{HI} DLAs are more homogeneously distributed in the redshift range than the high N_{HI} ones. The analysis for the redshift evolution gives a linear correlation coefficient much more significant for the low N_{HI} sample (-0.64 , 99.8% significance level) than for the high N_{HI} sample (-0.22 , 65.0% significance level), while the linear correlation gives a slope of $d \log Z_{DLA}/dz = -0.40 \pm 0.11$ and -0.14 ± 0.15 for the two samples, respectively. The fact that the metallicity for high N_{HI} DLAs is consistent with no evolution appears to be due to the high concentration of points in the central redshift range (70% are in the bin $2.0 < z < 3.1$). Indeed, the metallicity may

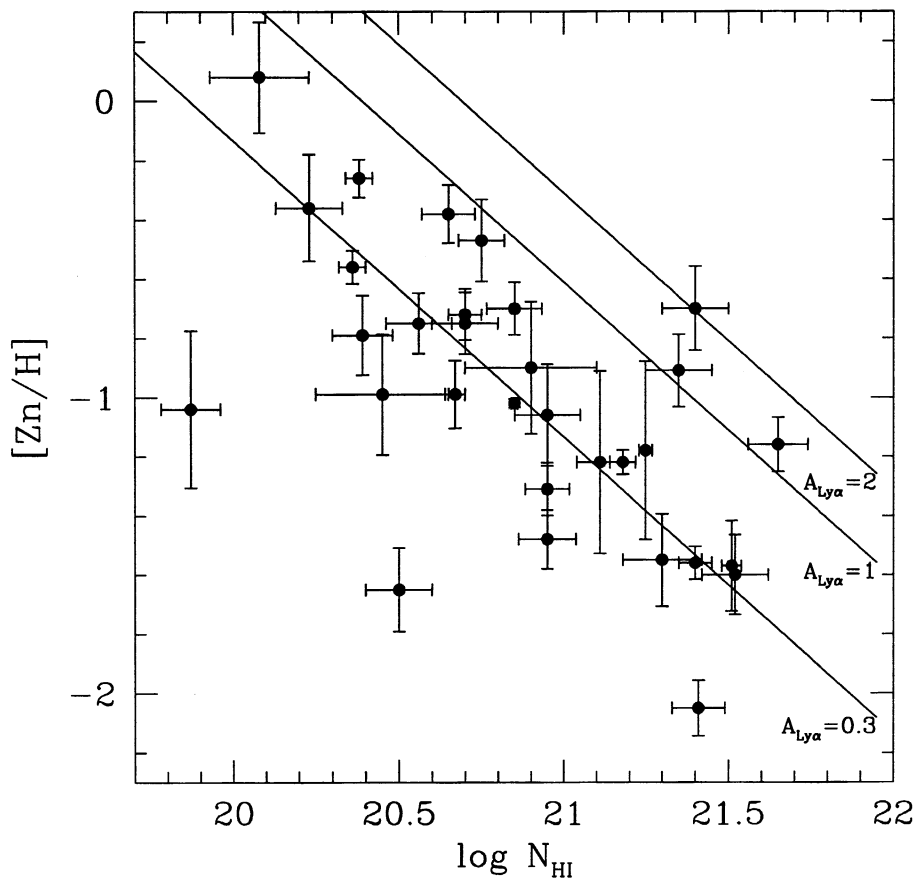


Figure 6. Zn abundance compared with solar as a function of HI column density in 31 DLAs. Straight lines are the $[Zn/H]$ and $\log N_{HI}$ values that give an extinction at Ly- α of 0.3, 1 and 2 magnitudes from the bottom to the top (SMC like extinction is assumed). These correspond to ZnII column densities of $\log N_{ZnII} = 12.5, 13.0, 13.3$ respectively.

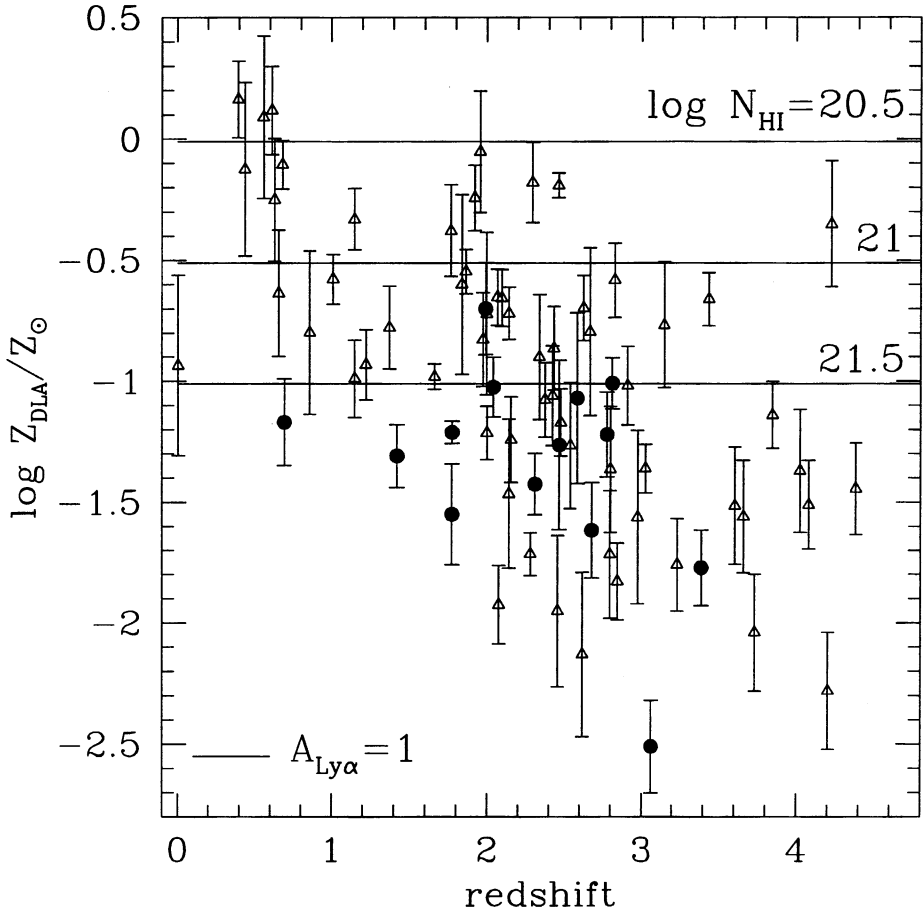


Figure 7. Same as Fig. 5, but triangles and dots are DLAs with $\log N_{\text{HI}} \leq 21$ and > 21 respectively. Horizontal lines indicate a 1 mag extinction at the Ly- α wavelength for three different HI column densities and metallicities. A SMC like extinction curve is assumed.

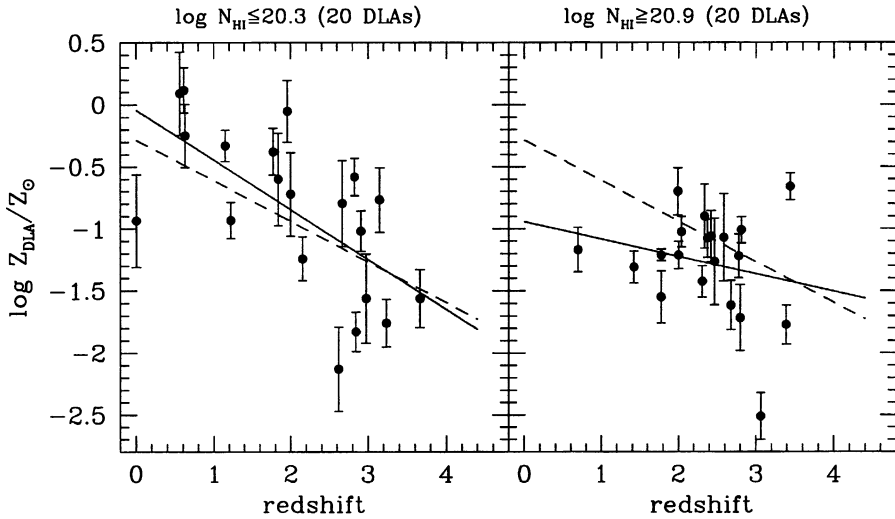


Figure 8. Same as Fig. 5, but for two subclasses of DLAs. On the left and right panels are 20 DLAs with $\log N_{HI} \leq 20.3$ and $\log N_{HI} \geq 20.9$ respectively. Solid lines are the linear correlation with $d \log Z_{DLA}/dz = -0.40 \pm 0.11$ (left panel) and $d \log Z_{DLA}/dz = -0.14 \pm 0.15$ (right panel). The dashed line in both plots is the linear correlation found in the whole sample of Fig. 5: $d \log Z_{DLA}/dz = -0.328 \pm 0.057$.

evolve just as rapidly as in the low N_{HI} clouds, as the two slopes differ only at the $\sim 2\sigma$ (95%) level. This has important consequences when considering the redshift evolution of the ratio of the total metal content to the total gas content, as we discuss in the next section.

6. Global Metallicity Evolution

The metallicity provided by DLAs is considered to be a good indicator of the global chemical evolution of the Universe. In particular this can be reproduced by the ratio of the total column density of metals to the total column density of gas of DLAs, i.e., $Z \propto \Sigma_i N_{met,i} / \Sigma_i N_{HI,i}$ (Pei & Fall 1995; Pei, Fall, & Hauser 1999). The ratio of the total metal content to the total gas content of DLAs in redshift bins has been calculated recently by Pettini et al. (1999) using 40 ZnII measurements, but these are actually 22 data points at $0.4 < z < 2.8$, if we exclude upper and lower limits. The so called ‘‘column density–weighted’’ metallicity obtained by these authors does not show any redshift evolution. Basically the same result has been obtained by Vladilo et al. (2000) using a larger ZnII database (27 ZnII measurements at $0.4 < z < 3.4$) and by Prochaska & Wolfe (2000) who have explored this quantity at higher redshifts using FeII instead (39 FeII measurements at $1.8 < z < 4.4$). If this analysis is done using our larger

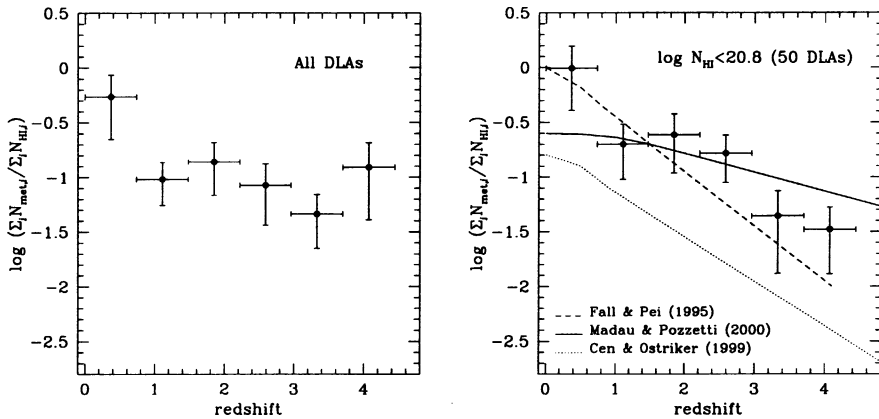


Figure 9. Ratio of the total metal content to the total gas content as a function of redshift. In the left panel the whole DLA sample is used, whereas in the right panel the subsample of DLAs with $\log N_{HI} < 20.8$ is considered. Different curves in the right panel represent the global chemical evolution of the Universe obtained by different models.

sample (75 DLAs at $0.0 < z < 4.4$) the results are not different (left panel of Fig. 9).

Considering the discussion of the previous section, this is not surprising. DLAs with low and high HI column densities are not distributed in the same way; in particular, the latter subsample is less homogeneous in the redshift range than the former. This means that when we consider the total metals to total gas ratio, where the high N_{HI} DLAs have a much larger weight compared to low N_{HI} DLAs, at low redshifts ($z < 1.5$) the metallicity is underestimated because high N_{HI} DLAs are preferentially detected when dust content, and therefore metallicity, is low (see Fig. 7). The detection of high N_{HI} DLAs is particularly hard in the redshift bin $z \sim 1$ because the observational capabilities are at the limits for both HST and ground-based telescopes. This is evident from Fig. 1, where the distribution of DLAs as a function of redshift has a hole in the interval $0.8 < z < 1.8$, also confirmed by the DLA selection function (the combined redshift survey path lengths for DLAs) reported by Mathlin et al. (2000). At high redshifts (7 DLAs at $z > 3.7$), the weighted metallicity is basically dominated by a single DLA at $z = 4.224$ (Prochaska & Wolfe 2000) with large HI column density ($\log N_{HI} \simeq 20.8$) and large metallicity ($[Fe/H] \simeq -0.35$, dust corrected). Indeed the column density weighted metallicity goes down to -1.5 if we exclude this DLA from the analysis.

The results change if we make a selection of DLAs using those which are likely to be less affected by dust obscuration. The total metals to total gas ratio in DLAs show evolution in the subsample of 50 DLAs with HI column density lower than 20.8 (right panel of Fig. 9). This goes from solar at $z \sim 0.4$ to $1/30$ solar at $z \sim 4.1$. For comparison we also plot the metal production in the Universe as given by the most recent results on the global star formation history of the Universe (solid line: Madau & Pozzetti 2000), and that obtained

using cosmological hydrodynamical simulations (dotted line: Cen & Ostriker 1999). The difference between these two behaviors is remarkable, both in the normalization and in the slope. The observed evolution has been reproduced by Pei & Fall (1995), who have used closed-box, inflow and outflow models with results similar to those used for the chemical evolution of the MW. These models were constrained by the very limited observational results known at that time on the DLA metallicity.

7. Discussion

It is not clear yet how well the mean HI weighted metallicity obtained from current observations can represent the global metal enrichment of the Universe because different observational biases might affect the results. As shown in Fig. 8, low and high N_{HI} DLAs are distributed in a different way (the latter are concentrated at the center of the redshift interval while the former are much more scattered). Moreover, the two correlations are consistent with each other at the $\sim 2\sigma$ level. The lack of high N_{HI} with high metallicity, theoretically first considered by Pei & Fall (1995) and then found by Boissé et al. (1998), might correspond to the lack of high N_{HI} DLAs at $z < 1.5$. If there were a metallicity evolution also for high N_{HI} DLAs, dust obscuration could be too large at $z < 1.5$ to make DLAs detectable (a DLA with $\log N_{HI} = 21.0$ and metallicity $\log Z_{DLA}/Z_{\odot} = -0.5$ would result in an extinction of about 1 magnitude at Ly- α). Moreover, this is where UV observations, required to detect Ly- α absorption, are very sensitive to any appreciable dust opacity.

In general, before using DLAs to explore the metallicity evolution in the Universe, one should understand if and how DLA galaxies represent the total galaxy population at different epochs. Obviously, this is not a trivial task because many factors have to be taken into account, some of which are very poorly known. When trying to match Lyman break galaxies to DLA galaxies, one should consider that the former are star forming galaxies for which the metallicity is usually inferred (and not measured) from the stellar and gaseous emissivity, while the latter are interstellar clouds with large HI column densities in galaxies of undefined nature for which the metallicity is measured from the absorption lines. On the other hand, when comparing DLAs with the intergalactic medium, one has to consider that high density regions like DLAs have very likely a different metallicity history than the mean value in the Universe and/or in the diffuse intergalactic medium. Cen & Ostriker (1999) have pointed out that higher density regions have higher star formation rates and after a fast heavy-element enrichment, the metallicity evolves very slowly compared to lower density regions, due to a suppression of star formation.

We like to stress that it is the combination of a large sample of DLAs (75 objects), a wide redshift baseline ($0.0 < z < 4.4$) and an accurate dust correction applied to all heavy elements measured, that has allowed us to demonstrate that the metallicity of DLAs evolves with redshift. Had we limited ourselves to using Zn only (detected in 31 DLAs) with no dust correction, we would have not detected the same effect, even if ZnII lines are known not to suffer from strong saturation and dust depletion. This is because even small corrections are important when trying to detect elusive effects. In addition, Zn is much

less abundant than other elements such as Fe and Si, and, therefore, measuring its absorption lines is not always an easy task. The combined use of as many elements as possible allows one to much more efficiently track the metallicity evolution down to gas clouds that are very metal poor.

Acknowledgments. I wish to thank the organizers of the IAU Symposium in Manchester, in particular Martin Harwit and Mike Hauser. I am grateful to Nino Panagia and Massimo Stiavelli for their important contribution at an early stage of the project.

References

- Boissé, P., Le Brun, V., Bergeron, J., & Deharveng, J.-M. 1998, *A&A*, 333, 841
- Cen, R., & Ostriker, J. P. 1999, *ApJ*, 519, L109
- Fan, X., et al. 1999, *AJ*, 118, 1
- Le Brun, V., Bergeron, J., Boissé, P., & Deharveng, J.-M. 1997, *A&A*, 321, 733
- Lu, L., Sargent, W. L. W., Barlow, T. A., Churchill, C. W., & Vogt, S. S. 1996, *ApJS*, 107, 475
- Madau, P., & Pozzetti, L. 2000, *MNRAS*, 312, L9
- Mathlin, G. P., Baker, A. C., Churches, D. K., & Edmunds, M. G. 2000, *MNRAS*, in press, astro-ph/0009226
- Pei, Y. C., & Fall, S. M. 1995, *ApJ*, 454, 69
- Pei, Y. C., Fall, S. M., & Hauser, M. G. 1999, *ApJ*, 522, 604
- Pettini, M., Smith, L. J., Hunstead, R. W., & King, D. L. 1994, *ApJ*, 426, 79
- Pettini, M., Smith, L. J., King, D. L., & Hunstead, R. W. 1997, *ApJ*, 486, 665
- Pettini, M., Ellison, S. L., Steidel, C. C., & Bowen, D. V. 1999, *ApJ*, 510, 576
- Prochaska, J. X., & Wolfe, A. M. 1999, *ApJS*, 121, 369
- Prochaska, J. X., & Wolfe, A. M. 2000, *ApJ*, 533, L5
- Rao, S., & Turnshek, D. A. 1998, *ApJ*, 500, L115
- Rao, S., & Turnshek, D. A. 1999, *ApJS*, in press, astro-ph/9909164
- Savage, B. D., & Sembach, K. R. 1996, *ARA&A*, 34, 279
- Savaglio, S., Panagia, N., & Stiavelli, M. 2000, in ASP Conf. Series, Cosmic Evolution and Galaxy Formation (San Francisco: ASP), astro-ph/9912112
- Spitzer, L. 1978, *Physical Processes in the Interstellar Medium* (New York: John Wiley & Sons)
- Vladilo, G., Bonifacio, P., Centurion, M., & Molaro, P. 2000, *ApJ*, in press, astro-ph/0005555
- Welty, D. E., Lauroesch, J. T., Blades, J. C., Hobbs, L. M., & York D. G. 1997, *ApJ*, 489, 672
- Wolfe, A. M., Turnshek, D. A., Smith, H. E., & Cohen, R. D. 1986, *ApJS*, 61, 249

Discussion

Charley Lineweaver: I am trying to understand what your $Z(z)$ results mean for the star formation rate. Does the Fall & Pei model you showed for $Z(z)$ (which fits your results) have a star formation rate which increases more steeply between redshifts 0 and 1 than most of the other rates we have seen over the last two days?

Sandra Savaglio: According to Michael Fall it does not. In fact, the cosmic star formation rate history in the Pei & Fall (1995) models is very similar to that inferred subsequently from the UV luminosity density history. In particular, the SFR in the Pei & Fall models also rises by about a factor of 10 between $z = 0$ and $z \sim 1$.

Richard Mushotzky: Most of the impact parameters are large, and so systematically sample outer, low-abundance regions of galaxies.

Michael Fall: A random distribution of impact parameters, with more impacts at large galactocentric distances, is just what one needs to get the mass-weighted mean metallicity, which is the same as the column-density-weighted mean metallicity. This is an unbiased measure of metallicity.

Savaglio: I agree.

Eli Dwek: What reference abundances did you use to correct for the depletions – solar or B-star abundances?

Savaglio: I don't expect to find different results, globally speaking.